Research on Engineering Structures & Materials
www.jresm.org
Research Group

Research Article

Phenomenological failure criteria analysis of a composite bolted joint under multi-axial loading using the finite element method

Manuela Karla Ribeiro Mathias[*,a], Bruno Mikio Fujiwara Marques[b]

Mechanical Engineering, Instituto Federal de Educação, Ciência e Tecnologia de São Paulo, IFSP, São José dos Campos, São Paulo, Brazil

Article Info

Article history:

Received 11 Apr 2024
Accepted 12 July 2024

Keywords:

Composites;
Bolted joints;
Failure criteria;
Hashin;
LaRC04;
Puck

Abstract

Carbon Fiber Reinforced Polymer Composites (CFRP) are commonly used in various sectors due to their excellent properties. However, they present complex failure modes, particularly in bolted joints, which are widely used in the aeronautical industry due to their ease of assembly and disassembly. Phenomenological failure criteria can be used to evaluate failure modes analytically and reduce the number of experimental tests. It is important to determine the criterion that best reflects reality. The Hashin, Puck, and LaRC04 failure criteria were evaluated using a finite element method software - FEMAP 2021.2 educational version - through simulation. Numerical simulations were conducted on a 2D model of a carbon/epoxy composite bolted joint under multiaxial loads, following ASTM D5661 dimensions. The failure criteria were compared to determine the most appropriate one for this type of component. Among the evaluated criteria, the Hashin criterion showed an intermediate level, while the Puck criterion was the most conservative and the LaRC04 criterion was the least conservative. It is recommended to use the Hashin criterion for general analyses. For analyses that require a detailed examination of compression failure modes, it is recommended to use the LaRC04 criterion. The Puck criterion is suggested for more conservative analyses.

1. Introduction

Carbon fiber reinforced polymer composites (CFRP) are widely used in the industrial sector due to their excellent properties, such as outstanding strength, high stiffness, and low weight [1, 2]. A notable example can be observed in the aerospace industry, where the Boeing 787 Dreamliner is composed of approximately 50% composite materials. As a result, the aircraft's weight is reduced, which consequently enhances its fuel efficiency [3, 4]. Moreover, these materials represent 40% of modern aircraft with a variety of applications, including interiors, engine blades, fuselage, wings, rotors, brackets, and others [1,4]. However, the failure modes for composite materials are complex due to the anisotropy and heterogeneity of the material, which depend on various factors such as the combination of fiber and matrix properties, the orientation of the fibers, and the number of plies in the component. As a result, they can present various types of damage mechanisms, such as delamination, fiber breakage, pull-out, matrix cracking, and other mechanisms, which makes it a challenge to identify the start of the failure [5, 6].

Therefore, it is necessary to take great care when manufacturing composite parts, especially bolted joints. Due to their ease of assembly and disassembly, bolted joints are crucial components in the aeronautical industry. However, despite this, more than 70% of

[*]Corresponding author: manuela.k@aluno.ifsp.edu.br
[a] orcid.org/0009-0005-2120-6918; [b] orcid.org/0000-0002-2367-9410
DOI: http://dx.doi.org/10.17515/resm2024.225me0411rs

structural failures occur at the joints [7,8]. In addition to the complexity of composite materials, the hole in their structure generates stress concentration in this region, making the components more susceptible to failures [7]. Thus, among the factors that can influence the failure mode of these components are the preload, the clearance of the screw hole, the type of screw head, and the geometric relationships between the hole diameter, width, thickness, and distance from the edge [9,10].

Generally, these components can fail in three main ways, varying based on the dimensions of the laminate: net-tension, shear-out, and bearing [10]. Net-tension and shear-out failures are the most catastrophic failure modes. While net-tension failure occurs at a low value for the ratio between the width of the plate to the diameter of the hole and a high value for the ratio between the distance from the hole to the edge of the joint by the diameter of the hole, shear-out failure occurs for reasons inverse to net tension, i.e., a high value between the width by the diameter and low value between the edge distance by the diameter [10]. However, unlike other failure modes, bearing failure produces a progressive failure. This failure is initiated by the compressive force applied to the inside of the hole by the bolt shank and a small value of the width-to-diameter ratio [9]. Due to the progressive failure behavior of bearing, bolted joints are designed to fail in this mode [7].

It is important to note that the application of torque is directly related to the resulting tension in the bolts and plates. Therefore, it is crucial to consider torque when studying bolted joints [7]. Torque generates a preload in the bolt, which aims to restrict the hole region and enable the transfer of external loads between plates through fixation [11]. The torque value should be defined based on the bolt strength, the material of the clamped parts and the type of installation so that the preload increases the strength of the bolted joint. Otherwise, if the torque is not properly applied, it could cause premature failure of the composite component due to the low resistance to out-of-plane stresses of these materials [7,9,10].

Furthermore, due to the wide range of factors that influence the failure modes of these components, the number of experimental tests has increased considerably, making material analysis costly, time-consuming, and analytically challenging [5,8]. This is particularly evident in the aerospace industry, due to the considerable costs and labor associated with the composites applied to this sector and the tools used in their production [3]. However, with increasingly powerful computers and the evolution of numerical modeling, simulation in software such as those using the finite element method (FEM) significantly reduces the number of tests, proving to be a cost-effective alternative when experimentally validated [2,3].

In conjunction with FEM simulation models, failure criteria for composite materials can be used to identify and predict the modes and onset of failure in the component being analyzed [5]. These criteria can be classified into macroscopic and microscopic aspects, with the macroscopic group being the most widely used due to their ease of application [12,13]. Within this group, there is a further classification grouping the criteria as follows [5,14]:

- Criteria that neglect the interactions between the different stress components, such as the maximum stress criterion and the maximum strain criterion.
- Criteria that include total stress interaction and have only one inequality, so they do not predict the initial failure mode, such as the Hoffman, Tsai-Wu, and Tsai-Hill criteria.
- Phenomenological criteria address the physical aspects of fracture and distinguish between different failure modes, such as the Hashin, Puck, and LaRC04 criteria.

The criteria in the third group, which deal with phenomenological models, are the closest to reality. Therefore, the study of these criteria is crucial for enhancing numerical analysis with accurate and realistic failure modes, especially in the industry, such as aircraft components, where the mechanical qualities are high and safety is of main concern. As the majority of commercial finite element software only provides the most traditional criteria, including Hashin, Tsai-Wu, Tsai-Hill, a limited number of studies have demonstrated the implementation of the Puck criterion used in the aeronautical sector [1,15]. Consequently, in addition to incorporating new criteria into the software, it is essential to validate them through experimental tests and identify the criterion that most closely aligns with reality for each component and specific conditions, with aim of reducing costs, time, materials and tests [1,13].

Good results using phenomenological criteria can be found in the literature. Zheng et al. [12] conducted a comparative study of failure criteria for predicting the onset of failure, concluding that the Hashin criterion provides reasonable results in a good execution time while the Puck and LaRC03 criteria offer more accurate results but with a longer execution time. Kober and Kühhorn [16] used the Tsai-Hill, Puck, and LaRC04 criteria to analyze, determining that the Puck criterion generates more realistic results. On the other hand, the LaRC04 criterion achieves results like the Puck criteria but from a mechanical point of view of the fracture. Marques et al. [13] carried out a comparative analysis between various criteria such as Hashin, Puck, Tsai-Hill, Tsai-Wu, Hoffman, and maximum stress, resulting in coherent results, but with an advantage for the Puck criterion due to the distinction between fiber and inter-fiber failure modes.

It is clear from the literature that the Puck criterion correlates well with experimental results, making it a reference for others [16]. The World-Wide Failure Exercise (WWFE) identified this criterion as one of the most effective in failure assessment [5]. In addition, several studies analyzing the results of FEM simulations of failure criteria for composite models compared to experimental results are available in the literature [1,15,17-20]. These studies present models with satisfactory results compared to their experimental tests.

In this context, a comparative analysis is proposed between the Hashin, Puck, and LaRC04 criteria, applied to a 2D model of a carbon/epoxy CFRP bolted joint in the FEMAP 2021.2 educational version software to determine the one best suits to this type of component. The model is a simple shear, two plates, and a bolt, subjected to multiaxial loads and dimensions according to ASTM D5961 [21].

2. Failure Criteria

The failure criteria employed in this study were consulted from the literature [5,13,15, 16,22], leading to the creation of Tables 1, 2, and 4, encompassing the equations for each criterion. In addition, some failure criteria depend on other constants and equations that may vary depending on the material and specimen analyzed.

In the equations, σ_1, σ_2, and σ_3 are the normal stresses in the principal axes of the specimen, τ_{12}, τ_{13} and τ_{23} are the in-plane and out-of-plane shear stresses, Xt and Xc are the longitudinal tensile and compressive strengths, Yt and Yc are the transverse tensile and compressive strengths, S_{12}, S_{13} and S_{23} are the in-plane and out-of-plane shear strengths, ε_1 is the normal strain, γ_{12} is the in-plane shear strain, m is the stress magnification factor, ε_{1t} and ε_{1c} are the longitudinal strain in tension and compression respectively.

Moreover, the failure modes are categorized as follows: fiber failure in tension (FFT), fiber failure in compression (FFC), matrix failure in tension (FMT), matrix failure in

compression (FMC), inter-fiber failure in transverse tension (IFF-A), inter-fiber failure in in-plane shearing (IFF-B), and inter-fiber failure in large transverse compression (IFF-C).

2.1. Hashin Criterion

Table 1. Hashin criterion equations [5,13]

FFT	$\left(\frac{\sigma_1}{X_t}\right)^2 + \frac{({\tau_{12}}^2 + {\tau_{13}}^2)}{S_{12}} = 1$	(1)
FFC	$-\left(\frac{\sigma_1}{X_c}\right) = 1$	(2)
FMT	$\frac{(\sigma_2 + \sigma_3)^2}{{Y_t}^2} + \frac{({\tau_{23}}^2 - \sigma_2\sigma_3)}{{S_{23}}^2} + \frac{({\tau_{23}}^2 + {\tau_{13}}^2)}{{S_{12}}^2} = 1 \text{ for } \sigma_2 + \sigma_3 > 0$	(3)
FMC	$\frac{1}{Y_c}\left[\left(\frac{Y_c}{2S_{23}}\right)^2 - 1\right](\sigma_2 + \sigma_3) + \frac{(\sigma_2 + \sigma_3)^2}{{Y_t}^2} + \frac{({\tau_{23}}^2 - \sigma_2\sigma_3)}{{S_{23}}^2} + \frac{({\tau_{23}}^2 + {\tau_{13}}^2)}{{S_{12}}^2} = 1$ for $\sigma_2 + \sigma_3 < 0$	(4)

2.2. Puck Criterion

Puck [23] determined the value of the inclination parameters (for further details, see [23]), and the parameters for CFRP materials are presented in Table 3. It should be noted that the parameter $P_{\perp\perp}^{-}$ exhibits a specified variation set at 0.30. Another constant, defined by the Puck criterion is the stress magnification factor (m), which accounts for the mismatch of elastic properties between the fiber and the matrix. For CFRP materials, its value is 1.1 [13].

Table 2. Puck criterion equations [13,15]

FFT	$\frac{1}{\varepsilon_{1t}}\left(\varepsilon_1 + \frac{\nu_{f12}}{E_{f1}} m\sigma_2\right) = 1 \text{ for } \left(\varepsilon_1 + \frac{\nu_{f12}}{E_{f1}} m\sigma_2\right) \geq 0$	(5)
FFC	$\frac{1}{\varepsilon_{1c}}\left\lvert\left(\varepsilon_1 + \frac{\nu_{f12}}{E_{f1}} m\sigma_2\right)\right\rvert + (10\gamma_{12})^2 = 1 \text{ for } \left(\varepsilon_1 + \frac{\nu_{f12}}{E_{f1}} m\sigma_2\right) < 0 \text{ and } \sigma_1 < 0$	(6)
IFF-A	$\sqrt{\left(\frac{\tau_{12}}{S_{12}}\right)^2 + \left(1 - P_{\perp\parallel}^{+}\frac{Y_t}{S_{12}}\right)^2\left(\frac{\sigma_2}{Y_t}\right)^2} + P_{\perp\parallel}^{+}\frac{\sigma_2}{S_{12}} + \frac{\sigma_1}{\sigma_{1D}} = 1 \text{ for } \sigma_2 \geq 0$	(7)
IFF-B	$\frac{1}{S_{12}}\left(\sqrt{(\tau_{12})^2 + \left(P_{\perp\parallel}^{-}\sigma_2\right)^2} + \left(P_{\perp\parallel}^{-}\sigma_2\right)^2\right) + \frac{\sigma_1}{\sigma_{1D}} = 1$ for $\sigma_2 < 0$ and $0 \leq \left\lvert\frac{\sigma_2}{\tau_{12}}\right\rvert \leq \frac{R_{\perp\perp}^{A}}{\lvert\tau_{12c}\rvert}$	(8)
IFF-C	$\left(\left[\left(\frac{\tau_{12}}{2(1 + P_{\perp\perp}^{-}S_{12})}\right)^2 + \left(\frac{\sigma_2}{Y_c}\right)^2\right].\frac{Y_c}{-\sigma_2}\right) = 1 \text{ for } \sigma_2 < 0 \text{ and } 0 \leq \left\lvert\frac{\tau_{12}}{\sigma_2}\right\rvert \leq \frac{\lvert\tau_{12c}\rvert}{R_{\perp\perp}^{A}}$	(9)

The longitudinal linear degradation index (σ_{1D}) is obtained experimentally, but as experimental tests will not be conducted, it will not be possible to obtain the linear degradation index, so two situations will be evaluated: the linear degradation index having a numerical value equal to the longitudinal stress (σ_1), with the ratio between the unknowns being equal to one; and the linear degradation index being significantly greater than the stress, with this ratio tending to zero.

Table 3. Inclination parameters [13]

Parameter	Value
$P_{\perp\perp}^{-}$	0.25 – 0.30
$P_{\perp\parallel}^{-}$	0.30
$P_{\perp\parallel}^{+}$	0.35

The longitudinal strain in tension (ε_{1t}) and compression (ε_{1c}) can be calculated as follows:

$$\varepsilon_{1t} = \frac{Y_t}{E_1} \tag{10}$$

$$\varepsilon_{1c} = \frac{Y_c}{E_1} \tag{11}$$

The terms $R_{\perp\perp}^{A}$ and τ_{12c} represent, respectively, the in-plane failure strength due to transverse or shear stress and the shear stress at the critical point where the transition between Mode B and Mode C occurs [15]. They can be calculated from the following equations [15]:

$$R_{\perp\perp}^{A} = \frac{S_{12}}{2P_{\perp\perp}^{-}}\left(\sqrt{1 + 2P_{\perp\parallel}^{-}\frac{Y_c}{S_{12}}} - 1\right) \tag{12}$$

$$\tau_{12c} = S_{12}\sqrt{1 + 2P_{\perp\perp}^{-}} \tag{13}$$

2.3. LaRC04 Criterion

Table 4. LaRC04 criterion equations [16,22]

FFT	$\frac{\sigma_1}{X_t} = 1$ for $\sigma_1 \geq 0$	(14)
FFC	$\left(\frac{\tau_{1m2m}}{S_{12is} - \eta^L \sigma_{2m2m}}\right)^2 = 1$ for $\sigma_1 < 0$ and $\sigma_{2m2m} < 0$	(15)
FFC[1]	$(1-g)\frac{\sigma_{2m2m}}{Y_{tis}} + g\left(\frac{\sigma_{2m2m}}{Y_{tis}}\right)^2 + \frac{\triangle_{23}^{0}\,\tau_{2m3\psi}^{2} + \chi(\gamma_{1m2m})}{\chi\left(\gamma_{\frac{12}{is}}^{u}\right)} = 1$ for $\sigma_1 < 0$ and $\sigma_{2m2m} \geq 0$	(16)
FMT	$(1-g)\frac{\sigma_2}{Y_{tis}} + g\left(\frac{\sigma_2}{Y_{tis}}\right)^2 + \frac{\triangle_{23}^{0}\,\tau_{23}{}^{2} + \chi(\gamma_{12})}{\chi\left(\gamma_{12/is}^{u}\right)} = 1$ for $\sigma_2 \geq 0$	(17)
FMC	$\left(\frac{\tau^T}{S^T - \eta^T \sigma_n}\right)^2 + \left(\frac{\tau^L}{S_{12is} - \eta^L \sigma_n}\right) = 1$ for $\sigma_2 < 0$ and $\sigma_1 \geq -Y_c$	(18)
FMC[2]	$\left(\frac{\tau^{Tm}}{S^T - \eta^T \sigma_n^m}\right)^2 + \left(\frac{\tau^{Lm}}{S_{12is} - \eta^L \sigma_n^m}\right) = 1$ for $\sigma_2 < 0$ and $\sigma_1 < -Y_c$	(19)

[1] Tensile failure of the matrix under longitudinal compression (with eventual fiber-kinking).

[2] Failure of the matrix under biaxial compression.

For the LaRC04 criterion, it is necessary to make some considerations regarding the behavior and dimensions of the specimen. According to Dvorak and Laws [22], the

transition between a thin and thick ply is between 0.7 mm, about 5 or 6 plies. Therefore, for the analysis, it was assumed that the specimen has a thick ply and is subjected to linear shear behavior. Knowing the laminate thickness, the transverse tensile strength (Y_{tis}) and the in-plane shear strength (S_{12is}) under the in-situ effect are calculated from the following equations [22]:

$$S_{12is} = \sqrt{2}S_{12} \tag{20}$$

$$Y_{tis} = 1.12\sqrt{2}Y_t \tag{21}$$

Additionally, for matrix failure under tension, the toughness ratio (g) was calculated using the Equation (14):

$$g = \frac{\triangle_{22}^{0} Y_{tis}^{2}}{\chi\left(\gamma_{12/is}^{u}\right)} \tag{22}$$

Thus:

$$\triangle_{22}^{0} = 2\left(\frac{1}{E_2} - \frac{\nu_{12}^{2}}{E_1}\right) \tag{23}$$

$$\chi\left(\gamma_{\overline{12}}^{u}\right) = \frac{S_{12/is}^{2}}{G_{12}} \tag{24}$$

The fracture angle (α) can be analytically calculated, so it was considered equal to 0º according to Pinho et al. [22], and the angle of fracture under uniaxial compression (α_o) based on experimental tests is generally equal to 53 ± 2º for composite materials, being defined as 53º for the application of the equations. These angles are applied to calculate some of the unknowns used in the equations of the LaRC04 criterion and are presented in more detail in Pinho et al. [22].

3. Failure Criteria Code

For the application of failure criteria in the FEMAP 2021.2 software – educational version - it was necessary to write the equations according to the software's programming. To achieve this, we used the guidelines described in the Function Reference document, accessed from the Help Topics option in FEMAP [25].

Table 5. Coding example: Hashin criterion - tensile fiber failure

Format	Written
Equation	$\left(\frac{\sigma_1}{X_t}\right)^2 + \frac{(\tau_{12}{}^2 + \tau_{13}{}^2)}{S_{12}} = 1$
Coded[1]	(SQR(VEC(!case;O1;!i)/Xt))+(((SQR(VEC(!case;T12;!i)))+(SQR(VEC(!case;T13;!i))))/SQR(S12))
Coded with properties (First Ply)	(SQR(VEC(!case;1000020;!i)/1006))+(((SQR(VEC(!case;1000023;!i)))+(SQR(VEC(!case;1000025;!i))))/SQR(68.1))

[1] O1=σ_1; τ_{12}=T12; τ_{13}=T13.

Initially, the properties of the composite material have been defined as parameters to make it possible to apply the coded equations to different materials. In addition, the stresses and strains were defined as vectors, because as they are associated with the model tested by the software, it is necessary to know the positions of the vectors for each of the stresses and strains generated by the software in post-processing. The parameters for vector positions and property values were substituted into the software. An example of the coding of the equations is in Table 5. The mechanical properties used in the analysis are of a

carbon/epoxy CFRP material produced by Gurit, SE 84LV RC416T [26] and are detailed in Table 6.

Table 6. Material and carbon fiber properties [13, 27]

Property	Value
Longitudinal modulus, E1 (GPa)	59.1
Transverse modulus, E2 (GPa)	58.9
Transverse modulus, E3 (GPa)	3.9
In-plane shear modulus, G12 (GPa)	4.2
Out-of-plane shear modulus, G13 (GPa)	4.2
Out-of-plane shear modulus, G23 (GPa)	22.7
Longitudinal tensile strength, XT (MPa)	1006
Transverse tensile strength, YT (MPa)	858
Longitudinal compressive strength, XC (MPa)	649
Transverse compressive strength, YC (MPa)	659
In-plane shear strength, S12 (MPa)	68.1
In-plane shear strength, S13 (MPa)	55.8
Major Poisson's ratio, ν12	0.037
Elastic modulus of the fiber, Ef1 (GPa)	231
Major Poisson's ratio of the fiber, νf12	0.28

The bolted joint was dimensioned according to the specifications of the ASTM D5961 standard, considering a simple two-piece shear test specimen without a fixing bracket [21]. The specimen was defined as having a thickness of 2.58 mm, divided into six plies of 0.43 mm each, and oriented $[0º/45º/90º]_S$. The dimensions are shown in Table 7 and illustrated in Fig. 1.

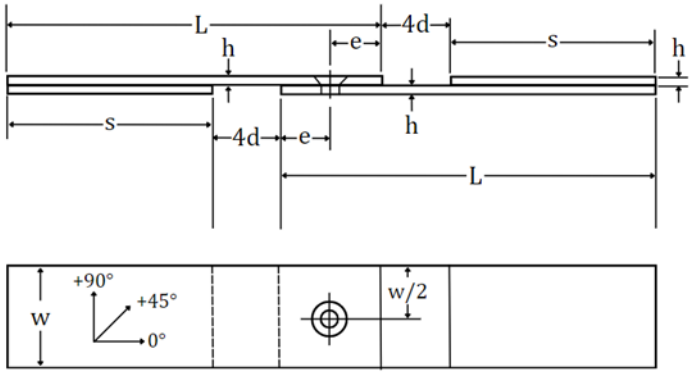

Fig. 1. Dimensions of the specimen [21]

Table 7. Dimensions of the specimen (mm) [21]

Hole diameter [d]	Length [L]	Width [w]	Edge distance [e]	Tab length [s]
6.35	135	36	18	75

The hole diameter was determined based on the NAS6204-4 standard [28]. According to the same standard, the bolt material was defined as AISI 4340 steels, and the mechanical properties of the material are in Table 8. To simulate the contact region, a washer with an outer diameter of 12.70 mm was used, following the NAS1149F0416P standard [29].

Table 8. AISI 4340 Steel property [30]

Property	Value
E1 (GPa)	210
ν12	0.28

To conduct the simulation, it was developed a 2D model of the bolted joint using FEMAP. The specimen's material was specified as 2D orthotropic, and the model property was divided into three sections: the left tab, the right tab, and the plate. Although the laminate plate property was defined in all three cases, the tab region, containing twice the number of plies, required specific definition and adjustment to accurately represent the specimen.

The left tab represents the region of the clamped end, while the right tab represents the region subjected to loading. Despite being a 2D model, it is possible to visualize the model considers the thickness of the specimen. Fig. 2 illustrates the model with the colors according to each property, and Table 9 shows the properties defined for each region of the model.

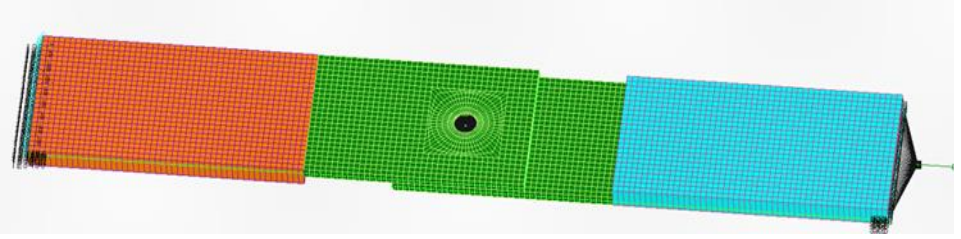

Fig. 2. Specimen model

Table 9. Properties applied to the model

Color	Number of plies	BondSh Allow (Mpa)	Ply configuration
10	6	55,8	0°/45°/90°/90°/45°/0°
14	12	55,8	0°/45°/90°/90°/45°/0°/0°/45°/90°/90°/45°/0°
120	12	55,8	0°/45°/90°/90°/45°/0°/0°/45°/90°/90°/45°/0°

The surface was discretized into 1.5 mm elements, resulting in 4604 elements and 14371 nodes after mesh refinement around the hole. Subsequently, two rigid elements (RBE2) were used to connect all nodes of each plate to a radius of 6.35 mm from the center of the hole to represent the washer in contact with the plates and the bolt. The bolt was represented by a beam element, which connected the RBE2s through the central node of each one.

However, the connections alone are not enough to represent the specimen, and it is necessary to establish a connection between them. The connection was made between the washers to link one plate to another. The connection type was set to contact, and properties were defined as standard by the software, with a coefficient of friction set to 0.3 [27]. Further details of the contact are illustrated in Fig. 3.

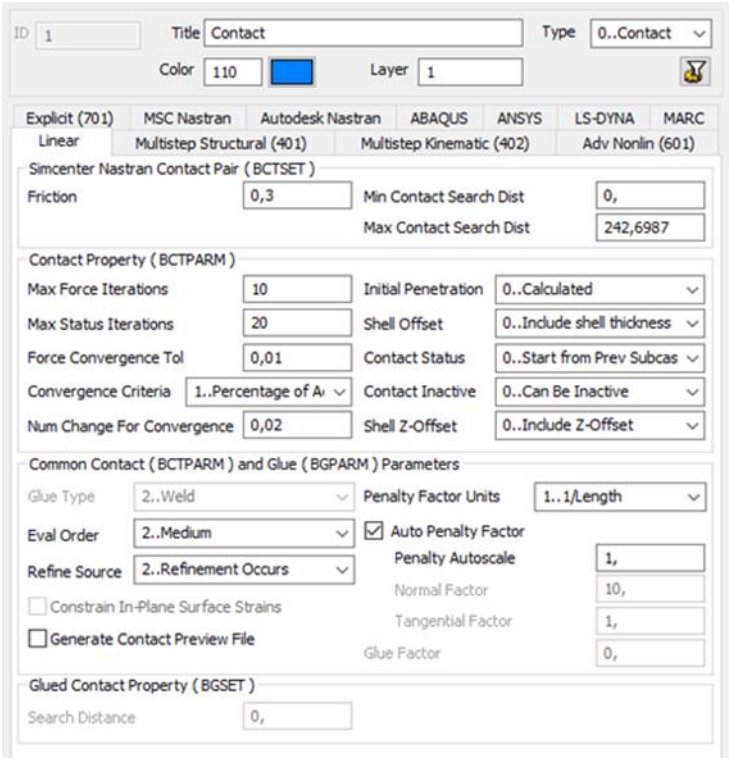

Fig. 3. Contact properties

Loadings were applied to a node outside the part, which transmits the load via an RBE2 to the nodes at the right end of the specimen. Eight loading cases were defined: 8000, 10000, 12000, 14000, 16000, 18000, 20000 and 22000 N. In addition, as the bolted joint is subjected to multiaxial loadings, a preload of 13124N was also applied in all loading cases. In order to calculate the pre-load using Equation (25) [10] the torque is set at 25 N.m and the torque coefficient at 0.3, based on the study by Marques [27], which showed that a torque of 25 N.m increases the mechanical strength of the joint without causing damage to the laminate.

$$F = \frac{T}{k.d} \tag{25}$$

Where F is the preload, k is the torque coefficient, T is the applied torque and d is the bolt diameter [10]. After simulating and adding the failure criteria equations to FEMAP, the failure indexes (FI) analysis was conducted, considering failure in the first ply. For each failure mode of each criterion, the element with the highest failure index in each ply was chosen. Then, the highest failure index among all plies was identified. Using the interpolation technique, loadings that closely approach the onset of failure were determined, with the failure index approaching the value 1. Consequently, the load values and the plies that failed were compared between the criteria to determine the criterion that best suits the behavior observed in the specimen.

4. Results and Discussion

After analyzing the failure index, Tables 10, 11, and 12 were generated, which show the loads at which the onset of failure was observed for each criterion in question, considering the failure of the first ply. In addition, no specific element in the model was considered, but rather the element that achieved the highest failure index, with the data interpolated to obtain a failure index equal to 1. The data was then put together in a line graph, illustrated in Fig. 4, providing a clear visual representation of the results obtained. For criteria with more than one compression failure mode, the lowest failure index was considered in the graphical representation.

Table 10. Hashin criterion - Loadings

Failure modes	Load (N)	Ply
Fiber failure in tension	15761	1
Fiber failure in compression	26032	6
Matrix failure in tension	18252	3
Matrix failure in compression	24904	2

Table 11. Puck criterion - Loadings

Failure modes	Load (N)	Ply
Fiber failure in tension	13839.07	6
Fiber failure in compression	26115.14	6
Inter-fiber failure in transverse tension (Mode A)	$\sigma_{1D} = \sigma_1$: 1000[1] $\sigma_{1D} >>> \sigma_1$: 4103.8	3
Inter-fiber failure in in-plane shearing (Mode B)	$\sigma_{1D} = \sigma_1$: 1000[1] $\sigma_{1D} >>> \sigma_1$: 5400.6	1
Inter-fiber failure in large transverse compression (Mode C)	4134.72	2

[1]Failure occurs at loads less than 1000N

Notably, the failure exhibits similar behavior between the criteria analyzed, such as Hashin and Puck. In plies 1 and 6, oriented at 0 degrees, fiber failure is observed, while in plies 2 and 3, at 45 and 90 degrees, respectively, matrix failure occurs. This is due to the fibers in the 0-degree direction being more resistant and supporting higher loads while in the 45 and 90-degree orientation, the matrix plays a supporting role, as the fibers are less resistant in these directions.

Furthermore, it was observed that tensile failures occur at lower loads compared to compressive failures. This behavior is related to the crushing failure mode of these components, as it generates compression in the region between the end and the edge of the hole. Therefore, as it is a progressive failure mode, it propagates slowly until failure

occurs. As tensile failure is a catastrophic failure mode, it is expected to occur at lower loads than compressive failure. Fig. 5 illustrates the mapping of stresses in the component, allowing precise identification of the areas where each type of failure occurs.

Table 12. LaRC04 criterion – Loadings

Failure modes	Load (N)	Ply
Fiber failure in tension	18229.3	1
Fiber failure in compression	39519.35	6
Fiber failure in compression[1]	46210.36	1
Matrix failure in tension	31037.45	1
Matrix failure in compression	29453.34	1
Matrix failure under biaxial compression	42132.17	1

[1] Tensile failure of the matrix under longitudinal compression (with eventual fiber-kinking);

*For Puck: Inter-fiber failure in transverse tension (Mode A)

** For Puck: Inter-fiber failure in large transverse compression (Mode C)

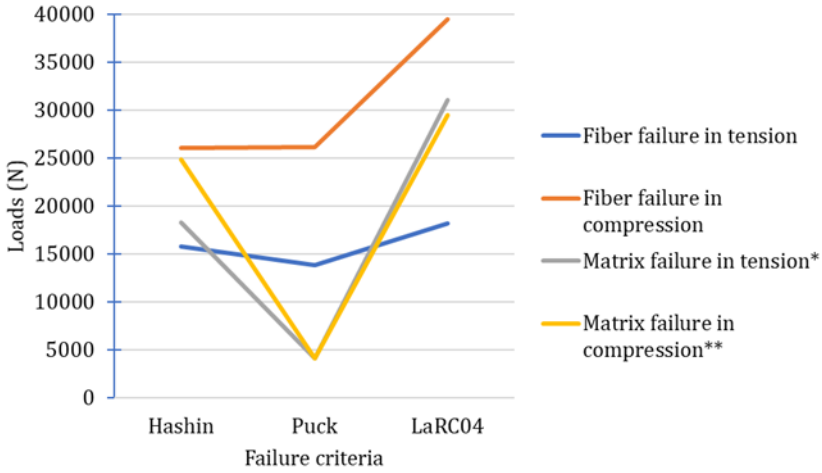

Fig. 4. Failure loads comparison

Similar results with experimental analysis are found in the literature, but it is important to highlight that are some differences due to the mechanical properties, orientations and the analysis method. Montagne et al. [31] studied the main parameters leading to the failure of joints based on an experimental database that included single-shear tests with countersunk head screws on various composite materials. They used Hashin's criterion for fiber failure and, based on the experimental results, found that some specimens failed in the net section, corresponding with Hashin's fiber failure criteria computed in the 0° plies. Additionally, the bearing failure mode was related to fiber failure in compression, delamination, or matrix damage, corresponding to failures in 0º or 45º plies due to fiber compression.

Park, Jeon, and Choi [32] studied the bearing strength of bolted joints in Carbon Fiber Reinforced Plastic (CFRP) with unidirectional weave fabric. They varied the specimen

width-to-hole diameter ratio and the distance between the hole center and specimen end-to-hole diameter ratio. For a width-to-hole diameter ratio of 6 and a distance-to-hole diameter ratio of 3, similar to the present work, the specimens experienced bearing failure.

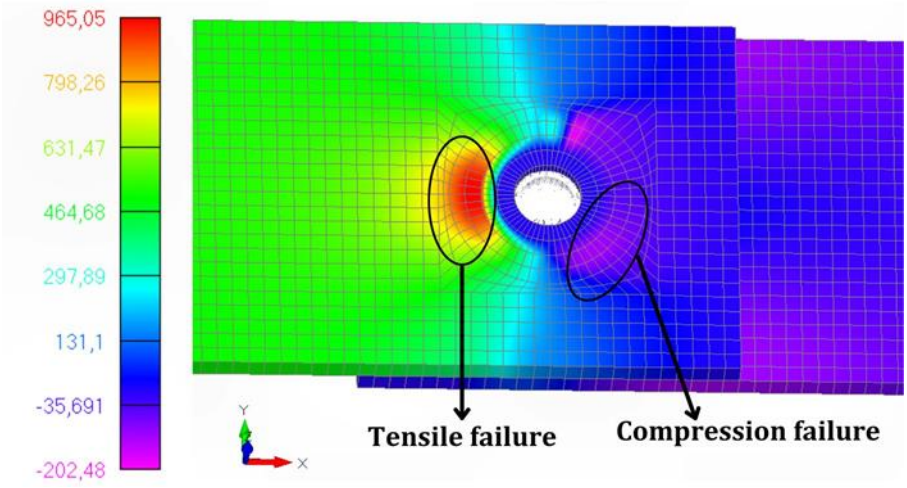

Fig. 5. Longitudinal stress map in ply 1 (0º), 18000 N and T0 model

Marques [27] studied the torque coefficients applicable to bolted joints in single shear overlays with two protruding head screws of carbon fiber reinforced epoxy matrix composite materials. The study examined the effects of different torque values on the laminate and demonstrated the relationship between bolt proof load and preload. Hashin's failure criteria was applied, which revealed interlaminar failure in the matrix, confirming the crushing effect and fiber failure in the longitudinal direction of the specimen due to traction. The results showed good correlation with the experimental tests.

About the criteria, Fig. 4 highlights that the matrix failure index for the Puck criterion occurs at significantly lower loads compared to the other criteria analyzed. Table 11 shows that for mode A and mode B the loads vary based on the value assigned to the linear degradation index, a material parameter that can be experimentally obtained. However, in the absence of experimental tests, the value was considered analytically. In the first case, it assumes that the linear degradation index value equals the longitudinal stress; consequently, the ratio between the parameters is 1. In the second case, the linear degradation index is considered much greater than the longitudinal stress, so the ratio between the parameters tends to be zero.

As a result, it is observed that for mode A, the tensile failure mode, in the first case, failure occurred at loads below 1000 N, while in the second case, failure was recorded at 4103.8 N. This type of failure, originating between the fibers, is associated with delamination between the plies and represents an initial failure mechanism because even with the presence of this mechanism, the component can withstand higher load levels [1, 13].

About mode B and mode C of the Puck criterion, both representing compressive failure mechanisms, Table 11 shows that they achieve a failure index equal to 1 in different plies and loads. In mode B, failure occurs in ply 1 at loads below 1000 N in the first case and at 5400.6 N in the second case. On the other hand, mode C results in failure in ply 2 with a load of 4134.72 N. This difference is due to the failure modes being associated with moderate and large compression, respectively. Thus, the region in which the equations are applied is limited by the ratio between the transverse stress and the in-plane shear stress,

and by the ratio between the strength of the failure plane and the critical transition point between mode B and C, as shown in Equations (8) and (9).

Despite being applied to different regions, modes B and C are characterized by the formation of cracks in the matrix, which propagate to the limits of the fiber, also representing an initial failure mode [1]. In this context, it is expected that both mode A and modes B and C, as they are initial failure mechanisms, will occur at lower loads, although in this case, they resulted in much lower loads than the other criteria.

As for the tensile and compressive fiber failure modes for Puck, the loads are close to the Hashin criterion. Puck is more conservative for tensile fiber failure, while Hashin is more conservative for compressive fiber failure, with a difference of approximately 100 N. Puck's more conservative behavior may be due to its equation, since it considers the failure plane, considering the micro-damage that occurs before the load reaches the material's strength, decreasing the strength of the matrix and increasing the chance of fiber failure [16].

On the other hand, the LaRC04 criterion behaves oppositely to the Puck criterion because failure occurs at much higher loads than the other criterion, especially in calculations involving compression, as shown in Table 12. The LaRC04 criterion considers the in-situ effect in its calculations, i.e., it considers the transverse tensile and shear strengths present in a ply of the laminate, limited by other plies of different fiber orientations [16, 22]. These strengths, as shown by Pinho et al. [22], are significantly higher when compared to unidirectional laminates. Therefore, due to the in-situ effect, it is expected that failure will occur at higher loads due to the greater resistance in the plies.

The in-situ effect is not considered only for tensile fiber failure which presents a more simplified equation, as shown in Equation (14). Fig. 4 shows that the discrepancy between the loads for which the failure index reaches 1 in this mode is smaller compared to the other modes, due to the greater similarity between the equations.

In addition, for the tensile failure of the matrix, the LaRC04 criterion occurs at a very high load and in a ply with a different orientation from the other criteria. For this failure mode, the LaRC04 criterion considers the ply stresses and in-situ strengths. However, it also considers the material's toughness coefficient, which can be obtained experimentally and analytically, based on Equation (22). However, after some comparisons, it was observed that the value calculated analytically is significantly higher than those obtained in the literature [16, 33]. Therefore, the coefficient may have influenced the results, causing the ply and the resulting load to vary.

As for the compressive failure modes, they can be divided into four failure modes, two of which are attributed to the fibers and two to the matrix. When analyzing the fiber failure modes by compression in the LaRC04 criterion, Table 12 shows that fiber failure by compression occurs at lower loads than tensile failure in the matrix under longitudinal compression (with eventual fiber kinking). Both are considered fiber failures, but they do have some differences. Fiber failure due to compression is related to kink-band formation, resulting in the phenomenon of micro buckling, while tensile failure in the matrix under longitudinal compression, with possible fiber kinking, relates two distinct types of failure: tensile failure in the matrix and fiber kinking due to deformation caused by shear in the matrix [22].

Regarding matrix failure, it is observed that matrix compression failure occurs at loadings lower than biaxial matrix compression failure. Biaxial compression failure considers fiber misalignment in its equations, while matrix compression failure considers the fracture plane [16]. Furthermore, biaxial matrix failure is related to fiber failure under

compression, resulting from micro buckling in the matrix and kink-band formation [Pihno21].

Finally, the Hashin criterion shows failure at intermediate loads. While the Puck criterion is associated with failure at low loads and the LaRC04 criterion is associated with failure at high loads. In addition, the Hashin criterion is subdivided into four failure modes, in which the failure is consistent with the orientation of the plies. It is important to note that to apply this criterion, all the material properties used were available, eliminating the need for analytical calculations to obtain them.

Also, it is important to note that, as the Hashin criterion was proposed first, the Puck and LaRC04 criteria that came later were based on some of its concepts [1,22]. Puck and his partners extended the Hashin criterion by dividing inter-fiber and fiber failure modes with the implementation of the fracture angle [1]. On the other hand, in the case of the LaRC04 criterion, the most recent of those discussed, it is developed from the fracture mechanics point of view [16,22].

Regarding failure criteria, several studies in the literature have utilized and compared different approaches. Dogan et al [34] investigated the failure behavior of carbon fiber reinforced pin-jointed composite plates using Hashin and Puck criteria. Compared with the experimental results, the numerical data using the Puck damage criterion showed at least 87% compatibility, while the Hashin damage criterion showed 85% compatibility for a single pin joint. In this case, for a ratio equal to 3 in a single pin, bearing failure, inter-fiber failure in shear, and inter-fiber failure in plane shear occur for Puck, while matrix shear and fiber compression occur for Hashin.

Gao et al [35] studied the strength and failure modes of fastened composite plates under static tensile loading based on experimental bolted joint bearing tests. They compared these results with various progressive damage numerical modeling simulations, considering the effects of damage variables, subroutines, and the Puck, Hashin, LaRC05, and maximum-stress criteria. The LaRC05 and Puck criteria provided more accurate results than the maximum stress and Hashin criteria in predicting matrix failure.

It is important to emphasize that some parameters used can be experimentally obtained for greater accuracy in the results. However, as it is not within the scope of this work to carry out tests on the specimens analyzed, the theoretical values were considered. Therefore, this variation in very high or very low failure index may be related to the considerations made when applying the criterion.

5. Conclusions

The FEMAP 2021.2 Educational Version software was used to perform a computer simulation of a bolted carbon fiber composite specimen, focusing on three failure criteria, Hashin, Puck, and LaRC04, to determine which best represented the specimen analyzed.

Thus, it can be concluded that the analysis based on the failure of the first ply of the bolted joint model was successful, presenting satisfactory and consistent results for the failure indexes of each criterion. With respect to fiber orientations, a variation in failure modes was observed depending on the orientation of each ply, with a greater tendency for fiber failure in the 0º plies, while matrix failure occurred in the 45º and 90º plies.

Additionally, it has been observed that tensile failure occurs at lower loads than compression failure, which aligns with the progressive crushing failure mechanism of these components. In terms of failure criteria, the Puck criterion is more conservative for fiber tensile failure, while the LaRC04 criterion is less conservative. On the other hand, the Hashin criterion is the most conservative for fiber compression failure, while the LaRC04

criterion is the least conservative. It is important to note that these observations are based on the modes of failure for LaRC04. The Puck criterion, which has an initial failure mechanism, exhibits much lower loadings, while the LaRC04 criterion shows significantly higher loadings for both matrix tensile and compression failure.

Therefore, the choice of criterion that best suits this type of component will depend on how conservative and detailed the analysis needs to be. In general, it is recommended to apply the Hashin criterion for the analyses. For analyses that require a more detailed examination of compression failure modes, it is suggested to use the LaRC04 criterion. For more conservative analyses, the use of the Puck criterion is proposed. However, it should be noted that the Puck criterion has shown failures at very low loadings, so it is recommended to verify the results using experimentally obtained parameters.

Acknowledgement

The authors acknowledge the financial support received from the CNPq - National Council for Scientific and Technological Development.

References

[1] El Idrissi H, Seddouki A. Modelling of progressive damage in a notched carbon/epoxy composite laminate subjected to tensile loading using different assessment methods coupled with FEM. Fibers and Polymers. 2022 Nov 1;23(11):3146-62. https://doi.org/10.1007/s12221-022-0019-4

[2] González C, Vilatela JJ, Molina-Aldareguía JM, Lopes CS, LLorca J. Structural composites for multifunctional applications: Current challenges and future trends. Progress in Materials Science. 2017;89:194-251. https://doi.org/10.1016/j.pmatsci.2017.04.005

[3] Cepero-Mejias F, Phadnis VA, Curiel-Sosa JL. Machining induced damage in orthogonal cutting of UD composites: FEA based assessment of Hashin and Puck criteria. Procedia CIRP. 2019;332-7. https://doi.org/10.1016/j.procir.2019.04.241

[4] Borges C, Chícharo A, Araújo A, Silva J, Santos RM. Designing of carbon fiber-reinforced polymer (CFRP) composites for a second-life in the aeronautic industry: strategies towards a more sustainable future. Front Mater.2023;10. https://doi.org/10.3389/fmats.2023.1179270

[5] Nali P, Carrera E. A numerical assessment on two-dimensional failure criteria for composite layered structures. Compos B Eng. 2012;43(2):280-9. https://doi.org/10.1016/j.compositesb.2011.06.018

[6] Parambil NK, Gururaja S. Bridging micro-to-macro scale damage in UD-FRP laminates under tensile loading. Int J Mech Sci. 2019 Jul 1;157-158:184-97. https://doi.org/10.1016/j.ijmecsci.2019.03.039

[7] Olmedo Á, Santiuste C. On the prediction of bolted single-lap composite joints. Compos Struct. 2012 May;94(6):2110-7. https://doi.org/10.1016/j.compstruct.2012.01.016

[8] Li X, Li Y, Li F, Huang Z, Chen H. Failure analysis and experimental study on bolted composite joints based on continuum damage mechanics. Compos Struct. 2023 Jan 1;303. https://doi.org/10.1016/j.compstruct.2022.116274

[9] El-Sisi A, Hassanin A, Alsharari F, Galustanian N, Salim H. Failure behavior of composite bolted joints: review. CivilEng. 2022 Dec 1;3(4):1061-76. https://doi.org/10.3390/civileng3040060

[10] Yoon D, Kim S, Kim J, Doh Y. Study on bearing strength and failure mode of a carbon-epoxy composite laminate for designing bolted joint structures. Compos Struct. 2020 May 1;239. https://doi.org/10.1016/j.compstruct.2020.112023

[11] Hu J, Zhang K, Cheng H, Qi Z. An experimental investigation on interfacial behavior and preload response of composite bolted interference-fit joints under assembly and

thermal conditions. Aerosp Sci Technol. 2020 Aug 1;103. https://doi.org/10.1016/j.ast.2020.105917
[12] Zheng J, Maharaj C, Liu J, Chai H, Liu H, Dear JP. A comparative study on the failure criteria for predicting the damage initiation in fiber-reinforced composites. Mechanics of Composite Materials. 2022 Mar 23;58(1):125-40. https://doi.org/10.1007/s11029-022-10016-3
[13] Marques BMF, Marques TPZ, Silva F de A, Cândido GM, Rezende MC. Failure criteria assessment of carbon/epoxy laminate under tensile loads using finite element method: validation with experimental tests and fractographic analysis. Mechanics of Advanced Materials and Structures. 2023;30(6):1274-83. https://doi.org/10.1080/15376494.2022.2029984
[14] Gu J, Chen P. Some modifications of Hashin's failure criteria for unidirectional composite materials. Compos Struct. 2017 Dec 15;182:143-52. https://doi.org/10.1016/j.compstruct.2017.09.011
[15] Gadade AM, Lal A, Singh BN. Finite element implementation of Puck's failure criterion for failure analysis of laminated plate subjected to biaxial loadings. Aerosp Sci Technol. 2016 Aug 1;55:227-41. https://doi.org/10.1016/j.ast.2016.05.001
[16] Kober M, Kühhorn A. Comparison of different failure criteria for fiber-reinforced plastics in terms of fracture curves for arbitrary stress combinations. Compos Sci Technol. 2012;72(15):1941-51. https://doi.org/10.1016/j.compscitech.2012.08.007
[17] Demiral M, Tanabi H, Sabuncuoglu B. Experimental and numerical investigation of transverse shear behavior of glass-fibre composites with embedded vascular channel. Compos Struct. 2020 Nov 15;252. https://doi.org/10.1016/j.compstruct.2020.112697
[18] Topac OT, Gozluklu B, Gurses E, Coker D. Experimental and computational study of the damage process in CFRP composite beams under low-velocity impact. Compos Part A Appl Sci Manuf. 2017 Jan 1;92:167-82. https://doi.org/10.1016/j.compositesa.2016.06.023
[19] Zhuang W, Zhang H, Wang E, Chen S, Liu Y. A progressive damage model for carbon fiber-reinforced polymer laminates subjected to fastener pull-through failure. Compos Struct. 2023 Dec 15;326. https://doi.org/10.1016/j.compstruct.2023.117623
[20] Gu J, Chen P, Su L, Li K. A theoretical and experimental assessment of 3D macroscopic failure criteria for predicting pure inter-fiber fracture of transversely isotropic UD composites. Compos Struct. 2021 Mar 1;259. https://doi.org/10.1016/j.compstruct.2020.113466
[21] ASTM International. ASTM D5961/D5961M - Standard test method for bearing response of polymer matrix composite laminates. West Conshohocken, PA; 2003.
[22] Pinho ST, Dávila CG, Camanho PP, Iannucci L, Robinson P. Failure models and criteria for FRP under in-plane or three-dimensional stress states including shear non-linearity [Internet]. 2005.
[23] Puck A, Kopp J, Knops M. Guidelines for the determination of the parameters in Puck's action plane strength criterion. Compos Sci Technol [Internet]. 2002;62(3):371-8. https://doi.org/10.1016/S0266-3538(01)00202-0
[24] Puck A, Schürmann H. Failure analysis of FRP laminates by means of physically based phenomenological models. Compos Sci Technol [Internet]. 1998;58(7):1045-67. https://doi.org/10.1016/S0266-3538(96)00140-6
[25] Siemens Digital Industries Software Inc. Simcenter Femap versão educacional 2021.2. 2021. Femap 2021.2 Help: 4.2.4.2 Plane element properties.
[26] Gurit Ltd. SE84LV low temperature cure epoxy prepreg. Wattwill: Gurit; 2017.
[27] Marques BMF. Análise do coeficiente de torque e do pré-carregamento resultante em juntas aparafusadas de compósito polimérico reforçado com fibra de carbono [Tese (Doutorado)]. [Guaratinguetá]: Universidade Estadual Paulista; 2022.

[28] Aerospace Industries Association of America Inc. NAS6203 thru NAS6220: bolt, tension, hex head, close tolerance, alloy steel, short thread, reduced major thread dia., self-locking and non-locking, 160 KSI Ftu. Arlington: AIA; 2013.
[29] Aerospace Industries Association of America Inc. NAS1149 - washer, flat. Arlington: AIA; 2008.
[30] AZoM. AISI 4340 alloy steel (UNS G43400) [Internet]. 2012 [cited 2024 Jan 15].
[31] Montagne B, Lachaud F, Paroissien E, Martini D. Failure analysis of composite bolted joints by an experimental and a numerical approach. In: Proceedings of the 18th European Conference on Composite Materials (ECCM18); 2018 Jun 24-28; Athens, Greece. p. 1-8.
[32] Park SM, Jeon JH, Choi WJ. Study on bearing strength and failure modes of single bolted joint carbon/epoxy composite materials. Polymers (Basel) [Internet]. 2024;16(6). https://doi.org/10.3390/polym16060847
[33] Sebaey TA, Blanco N, Lopes CS, Costa J. Numerical investigation to prevent crack jumping in double cantilever beam tests of multidirectional composite laminates. Compos Sci Technol. 2011 Sep 9;71(13):1587-92. https://doi.org/10.1016/j.compscitech.2011.07.002
[34] Dogan C, Kaman MO, Erdem S, Albayrak M. Comparison of Hashin and Puck criterions for failure behavior of pin loaded composite plates. Materwiss Werksttech [Internet]. 2024 Mar 1;55(3):314-29. https://doi.org/10.1002/mawe.202300104
[35] Gao G, An L, Giannopoulos IK, Han N, Ge E, Hu G. Progressive damage numerical modelling and simulation of aircraft composite bolted joints bearing response. Materials. 2020;13(24). https://doi.org/10.3390/ma13245606